109 RADIATIVE OBSERVATIONS OF THE MARINE BOUNDARY LAYER ON THE COAST OF TASMANIA

Jonathan Gero* and Robert Knuteson
Space Science and Engineering Center, University of Wisconsin-Madison, Madison, WI

1. INTRODUCTION

The 2nd U.S. Department of Energy (DOE) Atmospheric Radiation Measurement (ARM) Mobile Facility (AMF2) is currently deployed at the Kennaook/Cape Grim Baseline Air Pollution Station (CGBAPS) on the northwestern tip of Tasmania, Australia, as part of the ARM CAPE-k field campaign (Mace 2024). The location enables the observation of Southern Ocean air that has had minimal recent anthropogenic influence. Figure 1 illustrates that air sampled in the baseline sector (190–280°) has typically spent the previous several thousand kilometers without contact with land (Humphries et al. 2022). The facility provides cloud and precipitation observations from a suite of ground-based remote sensors and in situ instruments (CGBAPS 2024). The science goals of the ARM CAPE-k field campaign are to better understand the cloud radiative effects and cloud feedbacks in this under observed region, in order to improve representation of aerosol and cloud processes of the Southern Ocean in climate models (Mace et al. 2023, Mallet et al. 2023, McFarquhar et al. 2021). The observations are taking place between April 2024 – September 2025 with a planned visit by the R/V Investigator off-shore in May 2025 (Investigator 2024).

The AMF2 instrument complement includes the ARM Marine Atmospheric Emitted Radiance Interferometer (M-AERI), which measures upwelling and downwelling thermal infrared spectral radiance with high accuracy. The Atmospheric Emitted Radiance Interferometer (AERI) was developed at the University of Wisconsin–Madison Space Science and Engineering Center using funding support from the DOE ARM program in the 1990s (Knuteson et al. 2004a,b). One of the unique capabilities of the M-AERI is the ability for elevation angle scanning in a plane perpendicular to the front face of the instrument (Minnett et al. 2001). The AERI (and M-AERI) technology was subsequently licensed by UW-Madison to the commercial company ABB, Inc. which fabricated a M-AERI for the DOE ARM program (Knuteson et al. 2010). At the CAPE-k field site, the M-AERI has been positioned on an elevated cliff edge with a clear view into the clean air sector in the Southern Ocean to the west. In this configuration, using the elevation angle scanning capability of the M-AERI, the instrument can obtain high time resolution profiles of the temperature and humidity over the ocean and vertically over the cliff edge with improved height resolved information content (Seo et al. 2022). We report initial observations from the M-AERI instrument from the first half of the CAPE-k field campaign with comparison to the ARM Balloon-Borne Sounding System (BBSS) radiosonde launches and coincident ARM met tower surface observations. We also will investigate the ability of M-AERI to estimate the local temperature lapse rate over the ocean using its unique angle scanning capability.

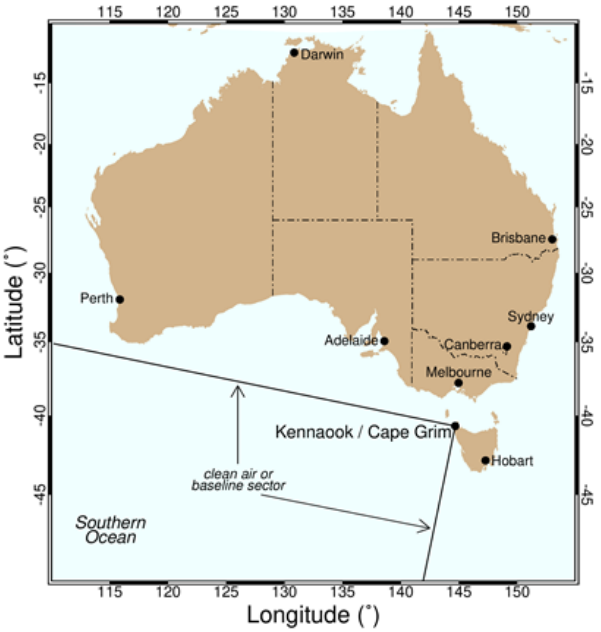


Figure 1. kennaook/Cape Grim Baseline Sector with relatively pure air from the Southern Ocean. Map is courtesy of CSIRO.

2. DATA AND METHODS

2.1 ARM Marine-AERI at CAPE-k

ARM AERI mentor J. Gero worked with the AMF2 and site operators to install the ARM M-AERI on a custom-built stand located within a few meters of the cliff edge with the scan plane oriented with azimuth of 260° from geographic north (247° magnetic) as illustrated in Figure 2. The AMF2 site is behind the M-AERI on a relatively flat area that slopes gently toward the cliff edge. Figure 3 shows the AMF2 site looking toward the cliff edge, the M-AERI is the white box in the distance on the left. This means the M-AERI location is at the lowest elevation of all the AMF2 observations (see Table 1), e.g. lower than the MET tower and BBSS locations indicated on Figure 2. These small elevation differences are important for data interpretation. The M-AERI installation is shown in Figures 4 and 5.

* *Corresponding author address*: Jonathan Gero, University of Wisconsin Space Science and Engineering Center, 1225 W Dayton St, Madison, WI 53706
E-mail: jonathan.gero@ssec.wisc.edu

Instrument	Latitude	Longitude	Elevation
M-AERI	-40.68071	144.68888	75 m
MET	-40.68075	144.68982	86 m
SONDE	-40.67839	144.69016	85 m

Table 1. Locations of instruments at the CAPE-k site

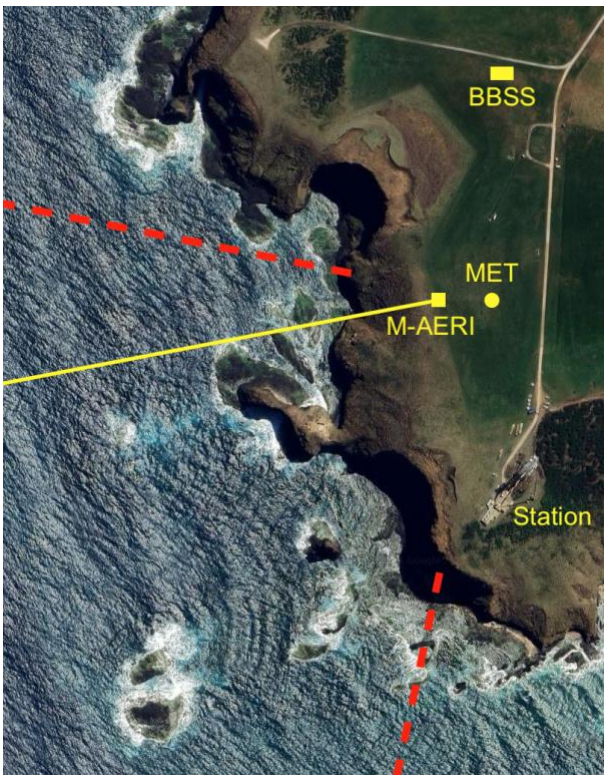


Figure 2. ARM AMF2 site layout at kennaook/Cape Grim. The M-AERI scanning plane azimuth is shown in yellow while the red dashed lines indicate the baseline sector.



Figure 3. View across CAPE-k AMF2 site toward M-AERI at cliff edge on the left. ARM photo.

The M-AERI has a programmable scan angle sequence which was configured specifically for the CAPE-k campaign. The M-AERI scan angle elevations of



Figure 4. ARM instrument mentor J. Gero works on a M-AERI installation near cliff edge. ARM photo.



Figure 5. M-AERI near cliff edge looking west over the Southern Ocean. ARM photo.

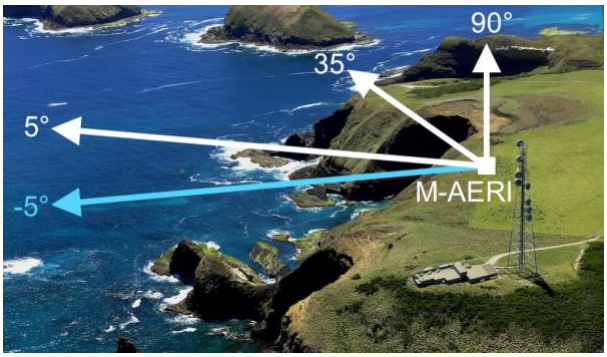


Figure 6. Illustration of M-AERI scan elevation angles.

-5°, +5°, +35°, and +90°, with respect to the horizon, used for this campaign are illustrated in Figure 6. The ±5° views are looking nearly horizontally over the ocean off the cliff edge. The +35° view provides an estimate of the downwelling flux from the atmosphere. The +90° view is consistent with the zenith views typically measured by non-scanning AERI instruments (Knuteson et al. 2004a, Feltz et al. 2003). The scan sequence is configured to

provide 8 zenith views interspersed with one sample view in each of the three non-zenith elevation angles as follows: [90°,90°,35°,90°,90°,5°,90°,90°,-5°,90°,90°]. The time period of the complete scan sequence is approximately 3 minutes and it repeats continuously from 0 to 24 UTC each day. The M-AERI has a hatch over the scene scan mirror that closes when triggered by a rain sensor and opens when the rain stops. A QC flag product is available for screening out data glitches.

The M-AERI measures thermal infrared spectra between 520–3020 cm^{-1} with a spectral resolution of 0.5 cm^{-1}. The ARM M-AERI *summary* file contains variables that are an average of radiance channels for three wavenumber ranges in each of the longwave (channel 1) and shortwave (channel 2) spectral bands. These radiances have been converted to the blackbody temperature that would be equivalent to that radiance for the selected wavenumber, i.e the so called brightness temperature (BT). Figure 7 shows the brightness temperature spectra for each scan angle for two time periods on 01 November 2024; 1) a period of positive lapse rate at the surface (21.5–22.5 UTC) and 2) a period of negative lapse rate (19.5–20.5 UTC). The vertical dashed lines indicate the wavenumber ranges used in the AERI summary files; 675–680 cm^{-1} (surface), 700–705 cm^{-1} (elevated), and 985–990 cm^{-1} (window).

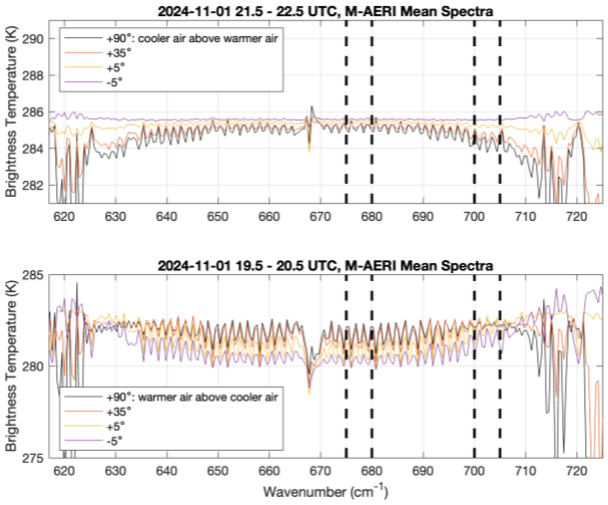


Figure 7. M-AERI brightness temperature spectra of the four scan view elevation angles for a time average of 21.5-22.5 UTC (top) and 19.5-20.5 UTC (bottom) on 01 November 2024.

The M-AERI data files used in this study were ordered from the DOE ARM archive in December 2024 (https://www.archive.arm.gov). The file *kcgaerisummaryM1.b1.20241101.000343.nc* is a netCDF file containing summary values of selected wavenumber ranges useful for making time series analyses. The variables used are *Time_UTC_hours*, *sceneMirrorAngle*, *surfaceLayerAirTemp675_680*, *elevatedLayerAirTemp700_705*, and *longwaveWindowAirTemp985_990*. The file *kcgaerich1M1.b1.20241101.000343.nc* is a netCDF file containing the time ordered radiance spectra for the longwave (channel 1) M-AERI band. The variable *all_mean_rad* contains the radiance spectra from all of the scan angles.

2.2 Penetration Depth

In order assign a distance range to the surface (675–680 cm^{-1}) and elevated (700–705 cm^{-1}) variables from the M-AERI summary file, the line-by-line infrared radiative transfer program LBLRTM v12.6 from AER, Inc. was used to estimate a nominal penetration depth. The penetration depth is defined as the depth at which the intensity of the radiation inside the material falls to 1/e, i.e. 0.368, of its initial value. Figure 8 shows the penetration depth computed at monochromatic spectral resolution for the U.S. standard atmosphere with a CO_2 mixing ratio of 330 ppmv. Note this is less than the current value of about 400 ppmv which would lead to greater absorption than shown. The average penetration depth for the surface variable has a range of 1 to 60 m with a mean value of 30 m. The average penetration depth for the elevated variable has a range of 10 to 350 m with a mean value of 150 m.

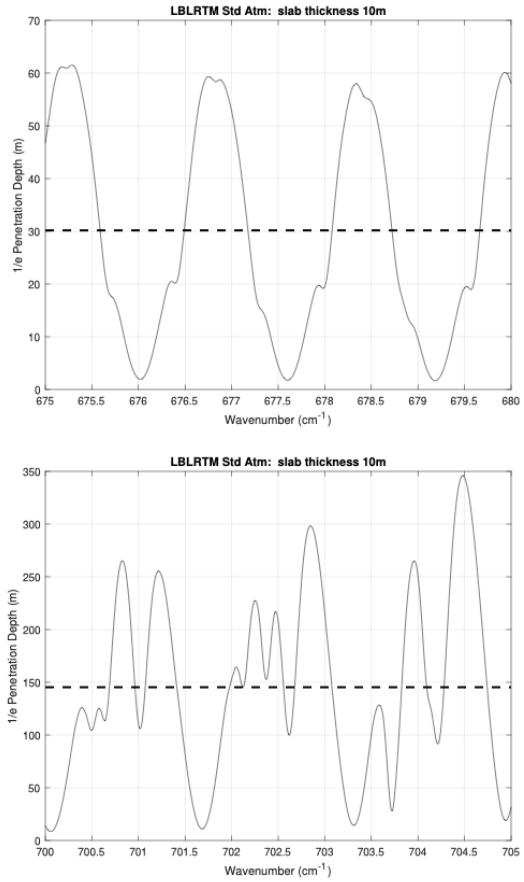


Figure 8. Penetration depth (1/e) for the *surfaceLayer* (top) and *elevatedLayer* (bottom) summary variables.

2.3 TROPoe Retrieval

The TROPoe (formerly called AERIoe) algorithm (Turner and Lohnert 2014, 2021; Turner and Blumberg 2019) retrieves profiles of temperature and water vapor mixing ratio, together with cloud properties for a single-layer cloud (i.e., LWP, effective radius), from AERI-observed infrared radiance spectra. The data can be used to characterize the evolution of the planetary boundary layer and boundary layer clouds. The TROPoe data files used in this study were ordered from the DOE ARM archive in December 2024 (https://www.archive.arm.gov). The file *kcgtropoeM1.c1.20241101.000502.nc* is a netCDF file containing the time sequence of vertical temperature and water vapor profiles derived only from the zenith (90° elevation angle) views. The slant elevation angle views are not retrieved with the operational version of the TROPoe algorithm, although in principle the methodology of Seo et al. 2022 could be used to process the M-AERI CAPE-k data in the future. In addition to the *height*, *temperature* and *waterVapor* variables, the TROPoe data file contains the planetary boundary layer height (*pblh*) and the surface-based inversion height (*sbih*).

2.4 Lapse Rate Estimation

The M-AERI installation at the cliff edge allows for a unique observation of the local temperature lapse rate over the ocean. The M-AERI was intentionally configured to obtain two near horizontal views at +5° and -5° elevation. The hyperspectral radiance at these view angles are sensitive to thermal emission from a range of distances from 1 m to more than 10 km depending on the optical depth of the spectral channel. The downlooking view at -5° angle intersects the ocean surface at a distance of approximately 860 m (M-AERI altitude / sin(5°)) while the uplooking view at +5° is through the marine boundary layer to the base of any low cloud in the distance. The assumed M-AERI observation altitude above the ocean surface is 75 m. The vertical separation between these two views of course varies from zero at the M-AERI sensor face to twice the M-AERI altitude at the point where the downlooking view intersects the ocean. As a first attempt to estimate the lapse rate from these views we have used the brightness temperature from the 700–705 cm^{-1} (elevated) variable from the M-AERI summary file, which has a penetration depth (i.e. distance range) of about 150 m. The vertical temperature lapse rate is defined to be the brightness temperature at the -5° view minus the +5° view divided by the absolute value of the altitude separation, $2\sin(5°) * 150\ m = 26\ m$. This follows the meteorological convention of decreasing temperature with height as a positive lapse rate and a negative lapse rate corresponds to a surface temperature inversion. The lapse rate computed as a difference of brightness temperatures is relatively immune to sensor calibration bias. The main uncertainty in the lapse rate calculation is from the estimate of the altitude separation of the views which depends on a proper understanding of the penetration depth (or other more appropriate measure of range).

2.5 ARM BBSS Radiosondes

The radiosonde data used in this study are from the ARM BBSS wnpn product downloaded from the ARM archive. The filenames are *kcgsondewnpnM1.b1.20241101.053000.cdf*, *kcgsondewnpnM1.b1.20241101.113000.cdf*, *kcgsondewnpnM1.b1.20241101.173000.cdf*, and *kcgsondewnpnM1.b1.20241101.233000.cdf*. The variables used are *time*, *alt*, *tdry*, *wspd*, and *deg*. Note that the *alt* variable is understood to be a GPS altitude from the Vaisala radiosonde and is therefore an independent observation which may not be consistent with mean sea level altitude or other measures of site elevation. Detailed instrument locations and elevations at the CAPE-k site is under review.

2.6 ARM Met Tower

The met data used in this study are from the ARM file *kcgmetM1.b1.20241101.000000.cdf* with variables *time*, *temp_mean*, *wspd_vec_mean*, and *wdir_vec_mean*. The nominal altitude of the met data is 86 m. The met tower wind direction observation is critical for the proper interpretation of the M-AERI observations at CAPE-k.

3. RESULTS

3.1 M-AERI Brightness Temperature

As described previously, the M-AERI summary file contains variables *surfaceLayerAirTemp675_680* and *elevatedLayerAirTemp700_705* that represent brightness temperatures at the nominal distances from the M-AERI scene mirror of about 30 and 150 m respectively. A third variable labelled *longwaveWindowAirTemp985_990* has a range limited only by cloud base for sky viewing angles or ocean in the downlooking angle. The time series of these variables are plotted in Figure 9 for the UTC date 01 November 2024 at the CAPE-k site. The BT of the individual scene views are shown in the four panels below; 90° (zenith), 35° slant sky view, 5° slant sky view, and -5° ocean view. Note the vertical scale of the lowest panel is different from the other panels. The black lines are the surface channel (675–680 cm^{-1}), the red lines are the elevated channel (700–705 cm^{-1}), and the blue line is the longwave window channel (985–990 cm^{-1}). We note that the longwave (LW) window time series of the sky views indicates cloud-free conditions when the BT is a minimum and the presence of cloud base in the field of view when the BT is greater than the minimum. The downlooking M-AERI view longwave window channel has a more complex interpretation which is deferred to the Discussion section. The same data is plotted in Figure 10 on an expanded a vertical scale that shows the small variations of the surface and elevated summary variables more clearly.

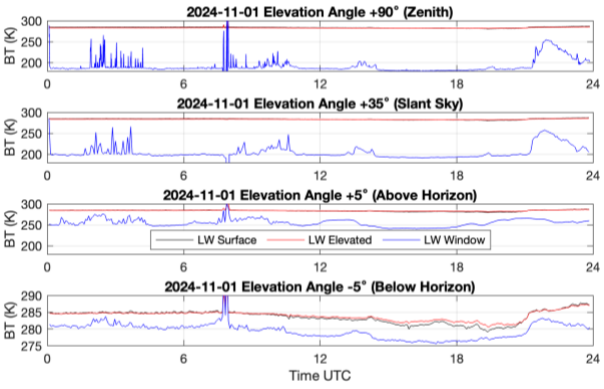


Figure 9. Time series of M-AERI summary variables for 01 November 2024.

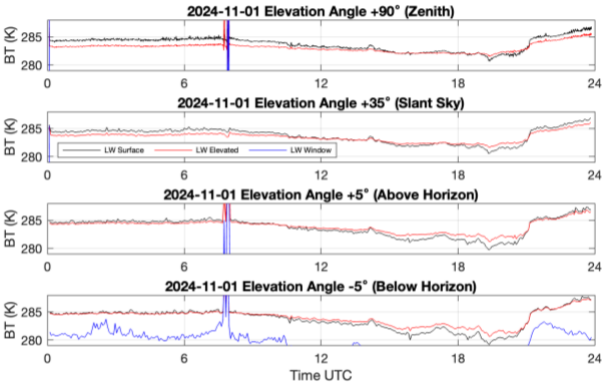


Figure 10. Same as Figure 9 but on an expanded vertical scale.

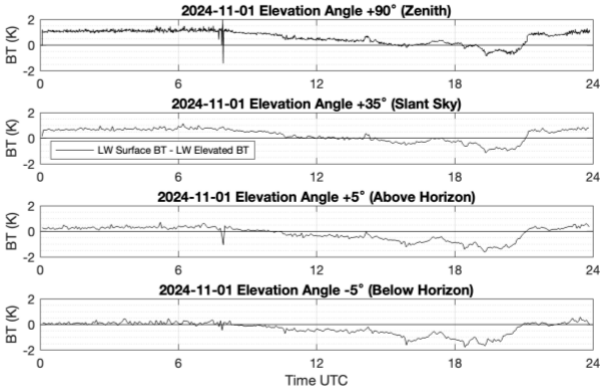


Figure 11. M-AERI LW Surface BT minus LW Elevated BT difference time series for each view angle on 01 November 2024.

Note that at times the surface BT is warmer than the elevated BT and at other times the reverse is true. In order to illustrate this variation with time, Figure 11 shows the surface BT minus the elevated BT as a time series for the four lower panels. When the BT difference is positive it indicates that the air nearest the M-AERI is warmer than the air farther away, and when the difference is negative the air near the M-AERI is cooler than the air farther away.

3.2 TROPoe

As previously described, the M-AERI zenith view radiances have been used to retrieve temperature and water vapor profiles using the TROPoe algorithm. The result from the TROPoe product file is shown in Figure 12 as time-height cross-sections. Note that this is a near real-time product produced by ARM operations using automated post-processing and as such has not been optimized for the CAPE-k site. The planetary boundary layer height (*pblh*) variable is shown as black dots. The *sbih* variable is plotted as red dots and indicates a surface inversion detected in the TROPoe profiles.

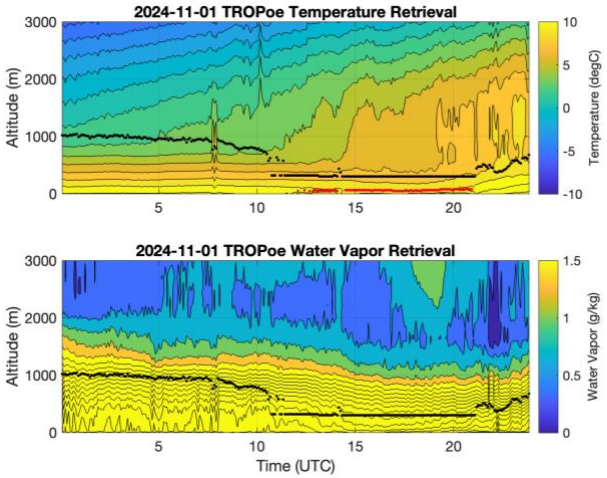


Figure 12. TROPoe time-height cross-section for temperature in Celsius (top) and water vapor mixing ratio in g/kg (bottom). The black dots are the *pblh* and the red dots are the surface inversion.

3.3 Sensor Intercomparison

Four ARM radiosondes were launched at CAPE-k on 01 November 2024 at 05:30, 11:30, 17:30, and 23:30 UTC. The BBSS launch site is indicated on Figure 2. The radiosonde temperature profiles are shown in Figure 13 plotted versus the radiosonde *alt* variable. From left to right in Figure 13, the radiosonde times are 17:30, 11:30, 5:30, and 23:30. The 5:30 and 23:30 UTC are during the daytime and the 11:30 and 17:30 UTC are at nighttime. Overlaid on the radiosonde profiles are the time coincident TROPoe retrievals plotted using the TROPoe height variable converted to altitude using the assumed M-AERI elevation of 75 m. In a similar way, altitudes have been assigned to the M-AERI brightness temperature variables for each view angle and are shown as symbols in Figure 13. The height assignment of the M-AERI BT values is using the penetration depth calculation from the previous section which is only a crude approximation and

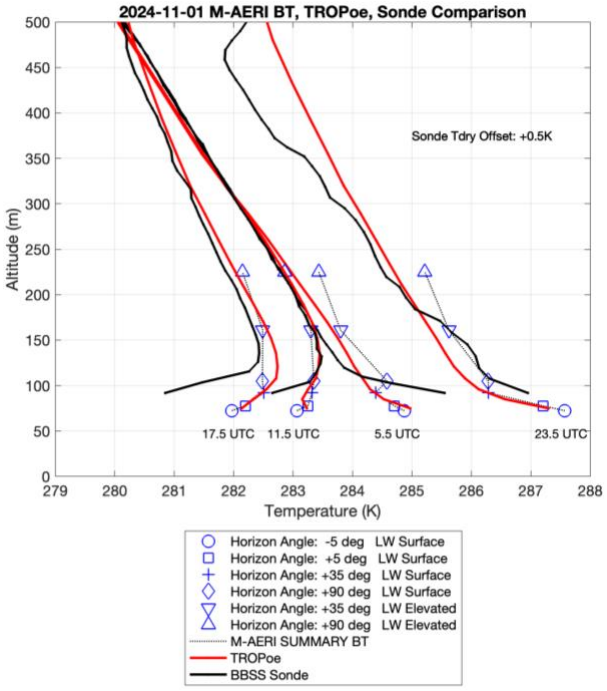


Figure 13. Overlay of time coincident profiles from radiosondes, TROPoe, and M-AERI BT.

subject to future revision. Each of the radiosonde temperature profiles have been shifted by +0.5 K to improve agreement with the M-AERI and TROPoe profiles. The source of this relative bias has not yet been identified and could equally be a bias error in the M-AERI real-time calibration of the opposite sign. Note that the BBSS system is launched from a location that is higher in altitude than the M-AERI which explains why the M-AERI and TROPoe profiles start at a lower altitude in Figure 13. Interpretation of these results is deferred to the Discussion section.

Figure 14 shows a comparison of the M-AERI BT timeseries with the ARM met tower temperature for 01 November 2024 along with coincident measurements of wind speed and direction from the ARM met tower on this date. The horizontal dashed lines on the top panel of Figure 14 indicate the baseline sector wind directions (190–280°) at the CAPE-k site. Note that when the wind direction departs from the baseline sector the M-AERI BT difference from the met tower changes sign, indicating a change in the horizontal and vertical distribution of air temperature over the AMF2 observation site.

3.4 Estimated Lapse Rate

As described in the Data and Methods section, the M-AERI radiometric scans at +5° and -5° elevation were used to estimate the temperature vertical lapse rate at about 150 m horizontal distance from the M-AERI over the ocean. The bottom panel of Figure 14 shows the lapse rate estimate as a timeseries compared to the wind speed and direction.

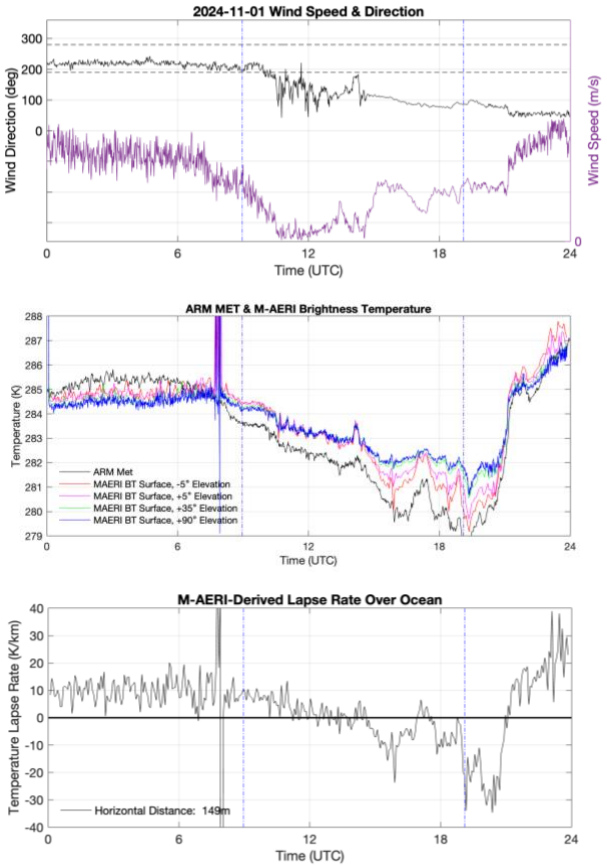


Figure 14. (top) wind direction and wind speed from ARM met tower observation. (middle) M-AERI brightness temperature time series overlaid with the ARM met tower air temperature. (bottom) M-AERI estimated vertical temperature lapse rate over ocean (150 m from cliff edge). Vertical dashed lines indicate sunset and sunrise.

4. DISCUSSION

The M-AERI scan angles shown in Figure 6 sample the atmosphere in a scanning plane oriented at 260° azimuth (10° south of due west). The M-AERI is the center of an arc of measurements sensitive to thermal emission at a range of distances. The measured emission is dependent on both the gaseous optical depth, which is wavenumber dependent, and the presence of a temperature gradient along the ray path. Figure 7 shows how the measured infrared emission varies with both scan angle and with the line structure of carbon dioxide as a function of wavenumber. Under the assumption of Kirchhoff's law of thermal radiation and the principle of detailed balance, the effective distance range of emission for each wavenumber channel can be estimated from the range of absorption, i.e. the penetration depth. This is a relatively crude assumption compared to the full radiative transfer theory used in the TROPoe algorithm, however it has proven useful for estimating temperature lapse rates near the M-AERI sensor.

Figure 14 shows that on 01 November 2024 the wind from 0–7 UTC is advecting air at about 8 m/s from within the baseline sector, from 7–11 UTC the wind speed drops to zero while the wind direction leaves the baseline sector and is coming from a southerly direction, from 11–21 UTC the wind speed increases steadily and the wind direction is coming from the southwest (influenced by land), at 21:30 UTC there is an abrupt increase in wind speed and the wind direction is coming from the east. At the same time, 0 UTC is 11 am local time during the daytime with sunset around 9 UTC (8 pm local) and sunrise around 19 UTC (6 am local) with daytime again until the end of the UTC date (10:59 am local next day). The interplay between the wind direction change, the day versus night heating/cooling, and the elevation differences among the sensor measurements must be considered in the interpretation of the results.

The M-AERI brightness temperatures shown in Figures 9 and 10 and the TROPoe retrievals in Figure 12 reveal how the atmospheric temperature structure changes in response to a change in wind direction. When the air is coming from the baseline sector the temperature lapse rate at and above the M-AERI altitude is positive and constant in time. When the when the wind direction comes from the land it is during the nighttime under clear skies. Under these conditions the low level air is cooler near the surface than the air above, this produces an increasingly strong surface temperature inversion. At 21:30 UTC an abrupt increase in surface air temperature is observed by the M-AERI and confirmed by the ARM met tower. This is followed by a period where the air is from the land but in the daytime so that the surface air is significantly warmer leading to a super-adiabatic temperature structure.

The influence of the breeze from the ocean and from the land is also seen in the behavior of the estimated lapse rate over the ocean shown in Figure 15. When the wind is from the baseline sector direction the results are stable and positive but when the wind is from the land influenced direction the lapse rate is impacted even as far as 150 m horizontally away from the cliff over the ocean.

4. CONCLUSIONS

The ARM CAPE-k field campaign started in February 2024 with the deployment of the ARM AMF2 and is expected to continue operating until September 2025. This paper highlights the preliminary measurements of the ARM Marine-AERI from a unique configuration at the Kennaook/Cape Grim Baseline Air Pollution Station. The M-AERI was installed with a scanning plane that views over the cliff edge of the sky and the ocean surface. Retrievals of temperature and water vapor from zenith views of the M-AERI are available from the ARM TROPoe product along with ARM BBSS radiosondes and ARM met tower data. Preliminary results are shown for a single date, 01 November 2024, which was selected to illustrate measurements for different wind directions, initially from the ocean baseline sector and then shifting to a direction that brought air from over land. The M-AERI views at +5° and -5° were used to estimate the temperature vertical lapse rate at a distance of about 150 m from the cliff edge. Future work includes analysis of intensive operating periods with up to eight radiosondes launched per day, including a planned period in May 2025 with the R/V Investigator offshore of the CAPE-k site.

Acknowledgments

This work has been supported in part by NASA ROSES grant 80NSSC22K1100 under the Decadal Survey Incubation Planetary Boundary Layer program. We acknowledge the support of the AMF2 team and technicians. Data were obtained from the Atmospheric Radiation Measurement (ARM) Program sponsored by the U.S. Department of Energy, Office of Science, Office of Biological and Environmental Research, Climate and Environmental Sciences Division.

References

Atmospheric Radiation Measurement (ARM) user facility. 2024. Atmospheric Emitted Radiance Interferometer (AERISUMMARY). 2024-04-15 to 2024-12-10, ARM Mobile Facility (KCG) kennaook／Cape Grim, Tasmania, Australia; AMF2 (main site for CAPE-k) (M1). Compiled by J. Gero, R. Garcia, D. Hackel, B. Ermold and K. Gaustad. ARM Data Center. Data set accessed 2024-12-13 at https://dx.doi.org/10.5439/1989300 .

CGBAPS, 2024. Kennaook/Cape Grim Baseline Air Pollution Station, URL: https://research.csiro.au/acc/capabilities/cape-grim-baseline-air-pollution-station/

Feltz, W.F., Smith, W.L., Howell, H.B., Knuteson, R.O., Woolf, H. and Revercomb, H.E., 2003. Near-continuous profiling of temperature, moisture, and atmospheric stability using the Atmospheric Emitted Radiance Interferometer (AERI). *Journal of Applied Meteorology*, *42*(5), pp.584-597.

Humphries, R.S., Keywood, M.D., Ward, J.P., Harnwell, J., Alexander, S.P., Klekociuk, A.R., Hara, K., McRobert, I.M., Protat, A., Alroe, J. and Cravigan, L.T., 2022. Measurement report: Understanding the seasonal cycle of Southern Ocean aerosols. Atmospheric Chemistry and Physics Discussions, 2022, pp.1-40. https://acp.copernicus.org/articles/23/3749/2023/

Investigator, 2024. RV Investigator. https://research.csiro.au/acc/capabilities/rv-investigator/

Knuteson, R. O., F. A. Best, N. C. Ciganovich, R. G. Dedecker, T. P. Dirkx, S. Ellington, W. F. Feltz, R. K. Garcia, R. A. Herbsleb, H. B. Howell, H. E. Revercomb, W. L. Smith, J. F. Short (2004a), Atmospheric Emitted Radiance Interferometer (AERI): Part I: Instrument design, *J. Atmos. Oceanic Technol.*, 21, 1763-1776.

Knuteson, R. O., F. A. Best, N. C. Ciganovich, R. G. Dedecker, T. P. Dirkx, S. Ellington, W. F. Feltz, R. K.

Garcia, R. A. Herbsleb, H. B. Howell, H. E. Revercomb, W. L. Smith, J. F. Short (2004b), Atmospheric Emitted Radiance Interferometer (AERI): Part II: Instrument performance, *J. Atmos. Oceanic Technol.*, 21, 1777-1789.

Knuteson, Robert; Best, Fred; Ciganovich, Nicholas; Garcia, Ray; Hackel, Denny; Revercomb, Henry; Taylor, Joe and Turner, David, 2010. E-AERI calibration performance certification. Multispectral, Hyperspectral, and Ultraspectral Remote Sensing Technology, Techniques, and Applications III, Incheon, Korea, 13-14 October 2010 (proceedings). SPIE-International Society for Optical Engineering, Bellingham, WA, 2010, Paper 78571L. Reprint # 6509.

Mallet, M.D., Humphries, R.S., Fiddes, S.L., Alexander, S.P., Altieri, K., Angot, H., Anilkumar, N., Bartels-Rausch, T., Creamean, J., Dall'Osto, M. and Dommergue, A., 2023. Untangling the influence of Antarctic and Southern Ocean life on clouds. Elem Sci Anth, 11(1), p.00130.

Mace, G. et al. 2023. Cloud and Precipitation Experiment at Kennaook (Cape-K) Science Plan. https://www.arm.gov/publications/programdocs/doe-sc-arm-23-011.pdf

Mace, G., 2024. CAPE-k: Cloud And Precipitation Experiment at kennaook, 15 April 2024 - 15 September 2025, Lead Scientist: Gerald Mace https://www.arm.gov/research/campaigns/amf2024cape-k

McFarquhar, G.M., Bretherton, C.S., Marchand, R., Protat, A., DeMott, P.J., Alexander, S.P., Roberts, G.C., Twohy, C.H., Toohey, D., Siems, S. and Huang, Y., 2021. Observations of clouds, aerosols, precipitation, and surface radiation over the Southern Ocean: An overview of CAPRICORN, MARCUS, MICRE, and SOCRATES. Bulletin of the American Meteorological Society, 102(4), pp.E894-E928.

Minnett, P.J., Knuteson, R.O., Best, F.A., Osborne, B.J., Hanafin, J.A. and Brown, O.B., 2001. The marine-atmospheric emitted radiance interferometer: A high-accuracy, seagoing infrared spectroradiometer. Journal of Atmospheric and Oceanic Technology, 18(6), pp.994-1013.

Seo, J., T. J. Wagner, P. J. Gero, and D. D. Turner, 2022. The Impact of Nonzenith Elevation Angles on Ground-Based Infrared Thermodynamic Retrievals. J. Atmos. Oceanic Technol., 39, 1395–1414, https://doi.org/10.1175/JTECH-D-21-0134.1.

Turner, D. D., and U. Löhnert, 2014. Information content and uncertainties in thermodynamic profiles and liquid cloud properties retrieved from the ground-based Atmospheric Emitted Radiance Interferometer (AERI). J. Appl. Meteor. Climatol., 53, 752–771, https://doi.org/10.1175/JAMC-D-13-0126.1.

Turner, D. D., and W. G. Blumberg, 2019. Improvements to the AERIoe thermodynamic profile retrieval algorithm. IEEE J. Sel. Top. Appl. Earth Obs. Remote Sens., 12, 1339–1354, https://doi.org/10.1109/JSTARS.2018.2874968.

Turner, D. D., and U. Löhnert, 2021.Ground-based temperature and humidity profiling: Combining active and passive remote sensors. Atmos. Meas. Tech., 14, 3033–3048, https://doi.org/10.5194/amt-14-3033-2021.